

# Simulation of a Perovskite Solar Cell with High Efficiency Using Various Hole Transport Layers

Souleymane Tuo<sup>1\*</sup>, Koffi Arnaud Kamenan<sup>2</sup>, Abou Bakary Coulibaly<sup>3</sup>

<sup>1</sup>Department of Physics, University of Man (U-Man), UFR Sciences and Technologies, Man, Côte d'Ivoire.

<sup>2</sup>Department of Mathematics, Physics and Chemical, UFR Biological Sciences, Peleforo Gon Coulibaly University (UPGC), Korhogo, Côte d'Ivoire

<sup>3</sup>New Energy Research Institute (IREN), Nangui Abrogoua University, Abidjan, Côte d'Ivoire  
Email: \*souleymane.tuo@univ-man.edu.ci

**How to cite this paper:** Tuo, S., Kamenan, K.A. and Coulibaly, A.B. (2025) Simulation of a Perovskite Solar Cell with High Efficiency Using Various Hole Transport Layers. *Crystal Structure Theory and Applications*, 13, 1-13.

<https://doi.org/10.4236/csta.2025.131001>

**Received:** August 25, 2025

**Accepted:** October 5, 2025

**Published:** November 27, 2025

Copyright © 2025 by author(s) and Scientific Research Publishing Inc. This work is licensed under the Creative Commons Attribution International License (CC BY 4.0).

<http://creativecommons.org/licenses/by/4.0/>



Open Access

## Abstract

Perovskite solar cells are the subject of numerous studies. These studies concern among others the optimal thickness and doping of the perovskite and the choice of charge transport materials. This work investigates the SCAPS simulation of a perovskite solar cell using separately SPIRO-OMeTAD, PEDOT:PSS, P3HT and Cu<sub>2</sub>O as the hole transport layer. The cell is completed with hematite as an electron transport layer. Thus, the simulation shows that the optimal thickness of the perovskite is around 700 nm and the optimal doping is 10<sup>20</sup> cm<sup>-3</sup>. Regarding the hole transport layers, we designed the influence of the thickness between 5 nm and 20 nm of these layers. It appears that over this range of thickness, the four HTLs contribute to obtaining almost equal performance of the cell with 35.21%, the maximum efficiency (PCE) obtained with PEDOT:PSS and 35.16%, the minimum PCE obtained with SPIRO-OMeTAD. However, this efficiency can reach over 42% by doping the perovskite layer at 10<sup>20</sup> cm<sup>-3</sup> NA. These promising results open the way to experimental trials to determine the real limits for this cell.

## Keywords

PSC, HTL, SCAPS, Thickness, Doping

## 1. Introduction

The diversification of materials in support of silicon is crucial to support the photovoltaic sector. It is known that silicon is the most widely used material in solar panels currently commercialized on the market. It represents about 90% of these panels [1]. Its theoretical limit efficiency (PCE) is 29.4% [2]. In this quest for di-

versification, perovskite is positioned as a promising material [3]-[7]. Several studies have announced interesting efficiency (PCE) exceeding 25.5% and comparable to those obtained with silicon [8]-[10]. For example, George G. et al achieved an impressive 37.67% (PCE) with a lead-free perovskite cell based on the ITO/PC61BM/CH<sub>3</sub>NH<sub>3</sub>SnI<sub>3</sub>/PEDOT:PSS/Mo configuration [11]. Olumide *et al.* reported that according to some authors, the efficiency of perovskite solar cells increased from 3.5% to 25.8% [12]. Also, Pratyush Panda *et al.* used two types of perovskites MASnI<sub>3</sub> and FASnI<sub>3</sub> together as active layers. They obtained a PCE of 28.06% [13]. If the choice of active material (absorber) is very important, it remains no less important the choice of materials for transporting loads. These are hole transport materials (HTM) and electron transport materials (ETM). The characteristics of perovskite solar cells are closely related not only to the nature of the perovskite, but also to the structure of the corresponding electron transport layer (ETL) and hole transport layer (HTL) [14]. Solar cells and particularly perovskite solar cells are built according to two configurations. The direct configuration (n-i-p) obeys the structure Substrate (glass)/Cathode (Al)/ETL/Perovskite/HTL/Anode (ITO) and the reverse configuration (p-i-n) follows the structure Substrate (glass)/Anode (ITO)/HTL/Perovskite/ETL/Cathode (Al) [15]. Indeed, instability at the interfaces is one of the many challenges for PSC perovskite solar cells without HTL in view of successful commercialization [16]. This work examines the influence of hole transport layers on cell performance. The use of a hole transport material (HTL) in perovskite solar cells is essential [17]. This layer presents a physical energy barrier between the anode and the perovskite layer that blocks the transfer of electrons to the anode, it also improves the efficiency of hole transfer [18]-[20]. Moreover, the HTL layer allows isolating the absorber from the metal electrode, thus curbing parasitic reactions (ion diffusion, corrosion), and can contribute to interfacial passivation [21]. For effective hole collection at the HTL/absorber interface, the valence band of the HTL should ideally be aligned with that of the absorber or have a slight shift ( $|V_{BO}| \leq 0.1$  eV), and to block electrons, the conduction band of the HTL should be considerably higher [22]. In this work, we want to study by designing with the SCAPS 1D software by comparing the influences of several HTL materials. It is about the PEDOT:PSS, P3HT, Cu<sub>2</sub>O and the SPIRO:OMeTAD. The study concerns the effect of the thickness, the concentration of doping of these materials on a perovskite solar cell with an ITO/ETL ( $\alpha$ -Fe<sub>2</sub>O<sub>3</sub>)/Perovskite/HTL structure (PEDOT:PSS, P3HT, Cu<sub>2</sub>O and the SPIRO:OMeTAD. Hematite  $\alpha$ -Fe<sub>2</sub>O<sub>3</sub> has been studied and shown its performance as an ETL [23].

The software SCAPS-1D was developed by Professor Burgelman and his team for electrical solar cell parameter design in fine layers. This was highly tested for solar cells based on CdTe, CIS and CIGS.

## 2. Methodology

### 2.1. Configuration of the Solar Cell

The perovskite solar cell simulated has a configuration with superposed layers.

Figure 1 presents this configuration.

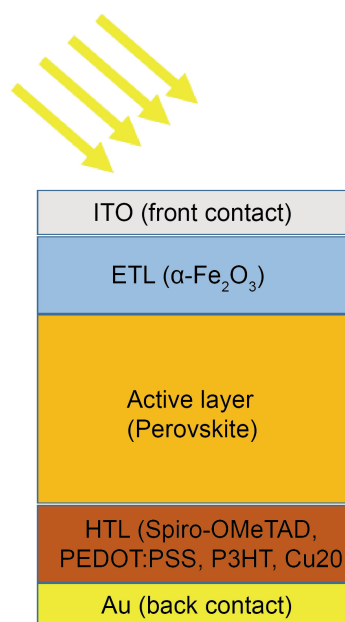


Figure 1. Configuration of solar cell.

## 2.2. Materials

In this study, we used the lead-free perovskite as an absorber layer (active layer). Then it is sandwiched between hematite ( $\alpha\text{-Fe}_2\text{O}_3$ ) the electron transport layer (ETL) and SPIRO-OMeTAD or PEDOT:PSS or P3HT or  $\text{Cu}_2\text{O}$  as the hole transport layer (HTL). The choice of hematite as ETL layer is justified by its abundance, chemical stability and transparency around 70% in the visible [24]. Several materials such as HTL were used to compare them with the cell's performance.

## 2.3. Methods

The SCAPS-1D software was developed by Professor Marc Burgelmann and his team was chosen to simulate the cell [25]. The optoelectronic properties of each material have been entered into the software. Table 1 gives the input values for

Table 1. Input value of each material.

Materials	$\text{CH}_3\text{NH}_3\text{SnI}_3$ [26]	$\alpha\text{-Fe}_2\text{O}_3$ [27]	PEDOT:PSS [28]	P3HT [29]	$\text{Cu}_2\text{O}$ [30]	Spiro-OMeTAD [31]
$E_g$ (eV)	2.3	1.3	2.2	1.8	2.17	3.2
$X$ (eV)	3.900	4.170	2.900	3.9	3.200	2.100
$\epsilon/\epsilon_0$	9.800	8.200	3.000	3.9	3.200	2.100
$N_c$ ( $\text{cm}^{-3}$ )	$3 \times 10^{18}$	$1 \times 10^{18}$	$1 \times 10^{15}$	3.000	7.5	3.000
$N_v$ ( $\text{cm}^{-3}$ )	$1 \times 10^{19}$	$1 \times 10^{18}$	$1 \times 10^{18}$	$1 \times 10^{19}$	$1 \times 10^{19}$	$1 \times 10^{19}$
$\mu_e$ ( $\text{cm}^{-2}/\text{Vs}$ )	$2 \times 10^{-3}$	$2 \times 10^{-3}$	$1 \times 10^{-1}$	$1 \times 10^{-5}$	20	$2 \times 10^{-4}$
$\mu_h$ ( $\text{cm}^{-2}/\text{Vs}$ )	$5 \times 10^{-5}$	$5 \times 10^{-5}$	$2 \times 10^{-3}$	0.2	80	$2 \times 10^{-4}$

## Continued

Nd (cm <sup>-3</sup> )	4.003 × 10 <sup>20</sup>		–			
Na (cm <sup>-3</sup> )		5 × 10 <sup>14</sup>	1 × 10 <sup>20</sup>	1020	1020	1020
Ve (cm/s)	1 × 10 <sup>7</sup>	1 × 10 <sup>7</sup>	1 × 10 <sup>7</sup>	10000	20	2 × 10 <sup>4</sup>
Vh (cm/s)	1 × 10 <sup>7</sup>	1 × 10 <sup>7</sup>	1 × 10 <sup>7</sup>	1 × 10 <sup>7</sup>	1 × 10 <sup>7</sup>	1 × 10 <sup>7</sup>
Doping Type	Neutral	Neutral	Neutral	Neutral	Neutral	Neutral
σ <sub>n</sub> (cm <sup>-2</sup> )	1 × 10 <sup>-15</sup>	1 × 10 <sup>-15</sup>	1 × 10 <sup>-15</sup>	1 × 10 <sup>-15</sup>	1 × 10 <sup>-15</sup>	1 × 10 <sup>-15</sup>
σ <sub>p</sub> (cm <sup>-2</sup> )	9.800	8.200	3.000	3.000	7.5	3.000
Energy distribution	Gaussian	Gaussian	Gaussian	Gaussian	Gaussian	Gaussian
N <sub>t</sub> (cm <sup>-3</sup> )	1. E+13	1. E+13	1. E+13	1. E+13	1.E+13	1.E+13

each material. These values are found in the literature. The simulation was done under AM1.5G illumination (1000 W/cm<sup>2</sup>), at a temperature of 300 K. We considered the ITO, with an output work function of 4.7 eV as the front contact and gold with an output work function of 5.1 eV as the back contact. In the simulation, we varied on the one hand the thickness of the perovskite layer between 100 nm and 1000 nm and on the other hand the doping varying between 1 × 10<sup>10</sup> cm<sup>-3</sup> and 1 × 10<sup>22</sup> cm<sup>-3</sup>. Then, the thickness of the charge transport layers of the holes varying between 5 nm and 20 nm was considered. The ETL layer made of hematite has not changed. Its thickness is set at 10 nm [26].

### 3. Results and Discussion

#### 3.1. Influence of the Active Thickness Layer on the Cell Parameters

To study the influence of the absorbing layer, we considered the perovskite solar cell with Spiro-OmeTAD as the hole transport layer and hematite as the electron transport layer. We set the thickness of the charge transport layers (ETL and HTL) at 10 nm each. **Figure 2** shows the influence of the thickness of perovskite layer on solar cell parameters (J<sub>sc</sub>, V<sub>oc</sub>, FF and PCE).

##### 3.1.1. Influence of the Active Layer Thickness on the Short-Circuit Current (J<sub>sc</sub>)

When the thickness of the perovskite varies from 100 nm to 1000 nm, the short-circuit current J<sub>sc</sub> changes from 20 mA/cm<sup>2</sup> to almost 35 mA/cm<sup>2</sup> and then stabilizes. It reaches this value from 700 nm. **Figure 2** illustrates the influence of the thickness of the perovskite on the short-circuit current. This evolution is consistent with the literature. Indeed, the increase in thickness improves photonic absorption in the visible and therefore the generation of electron-hole pairs [32] [33]. The thickness of 700 nm here seems to be the one that allows the absorption of almost the entire visible spectrum. What justifies the stability of the current at this thickness value.

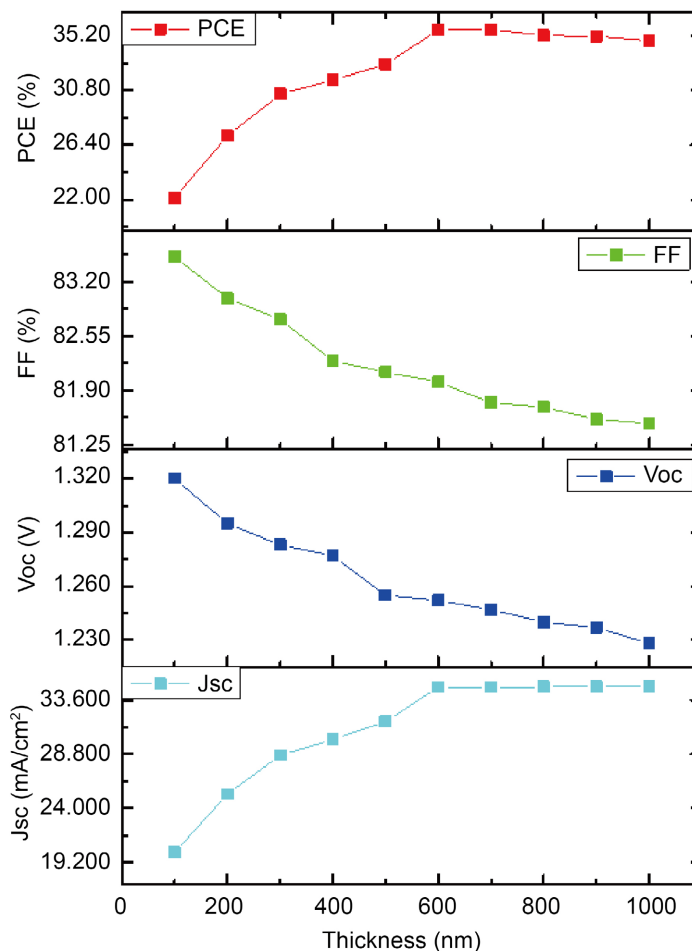


**Figure 2.** Influence of the thickness of perovskite layer on solar cell parameters (Jsc, Voc, FF and PCE).

### 3.1.2. Influence of the Active Layer Thickness on the Open-Circuit Voltage (Voc)

We notice in **Figure 2** that the Voc decreases from 1.32 V to about 1.23 V. This decrease results in an increase in recombination effects as the layer becomes increasingly thick [32], showing that any increase in thickness induces a drop in the open circuit voltage.

### 3.1.3. Influence of the Active Layer Thickness on the Fill Factor (FF)

**Figure 2** shows a moderate decrease in the fill factor from about 83.5% to 81.5%. This results in increased losses due to the resistance series and internal recombinations. Indeed, when the thickness of the active layer increases, the path of charge carriers lengthens and increases their probability of recombination [8] [33].

### 3.1.4. Influence of the Active Layer Thickness on the Power Conversion Efficiency (PCE)

In **Figure 2**, we can see that the efficiency increases from 20% at a thickness of 100 nm to practically 35% at 700 nm. This maximum value is reached as soon as the active layer (absorbent) reaches a sufficient thickness for an almost complete ab-

sorption of the visible spectrum while maintaining acceptable losses. These results confirm the existence of an optimal perovskite thickness around 700 nm, in agreement with experimental and numerical works which place this maximum between 400 and 800 nm depending on the carrier diffusion length and the crystalline quality of the absorber [8] [34] [35].

Furthermore, the use of  $\text{Fe}_2\text{O}_3$  as an electron transport layer (ETL) influences these results. Although abundant, stable and inexpensive,  $\text{FeO}$  generally exhibits a lower electron mobility than  $\text{TiO}$  or  $\text{SnO}$  generally used, and can absorb part of the blue spectrum [34]. Obtaining a high efficiency with this material requires an optimization of the interfaces (passivation, doping) to limit recombinations at the ETL/absorber interfaces.

## 3.2. Influence of HTL Thickness Layer on the Cell Parameters

### 3.2.1. Influence of HTL Thickness Layer on the Short-Circuit Current

It is observed in **Figure 3** that, when the thickness of the HTL layers varies from 5 nm to 20 nm, the short-circuit current ( $J_{sc}$ ) increases slightly from 33.948  $\text{mA}/\text{cm}^2$  to 33.949  $\text{mA}/\text{cm}^2$ ; 33.947  $\text{mA}/\text{cm}^2$  to 33.951  $\text{mA}/\text{cm}^2$ ; 33.947  $\text{mA}/\text{cm}^2$  to 33.948  $\text{mA}/\text{cm}^2$  for PEDOT:PSS, P3HT and  $\text{Cu}_2\text{O}$  respectively. It remains however constant at 33,947  $\text{mA}/\text{cm}^2$  for the SPIRO-OMeTAD. These results show that regardless of the HTL material, the short-circuit current varies slightly. This means that the HTL layers are thick enough to ensure the selectivity of holes and block electrons, but not thick enough to introduce recombination phenomena.

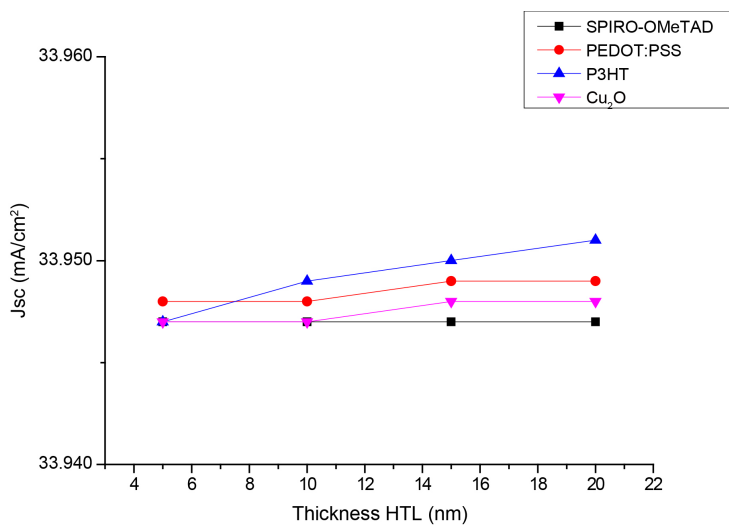


**Figure 3.** Influence of the thickness layer of HTL (SPIRO-OMeTAD, PEDOT:PSS, P3HT and  $\text{Cu}_2\text{O}$ ) on short-circuit current.

### 3.2.2. Influence of HTL Thickness Layer on the Open Circuit Voltage

In **Figure 4**, the open circuit voltage ( $V_{oc}$ ) is constant at 1.243 V for SPIRO-OMeTAD and P3HT and 1.244 for PEDOT:PSS, and  $\text{Cu}_2\text{O}$ . It clearly appears that the  $V_{oc}$  values are almost equal for all four HTL used. This suggests that this thickness range does not strongly influence the open circuit voltage.

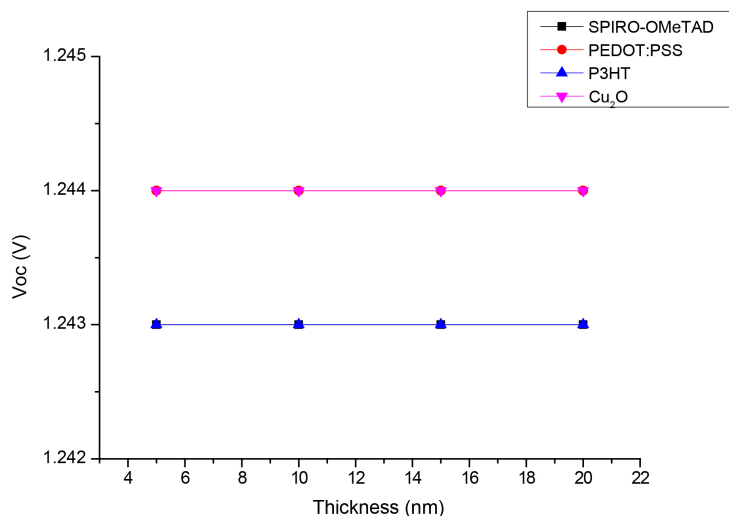


**Figure 4.** Influence of HTL thickness layer (SPIRO-OMeTAD, PEDOT:PSS, P3HT and Cu<sub>2</sub>O) on open circuit voltage.

### 3.2.3. Influence of HTL Thickness Layer on the Fill Factor

The fill factor (FF) displays practically constant values with slight shifts between the different HTL as we can observe in **Figure 5**. The best form factor, 83.41% is obtained with P3HT, followed by PEDOT:PSS, 83.37%. The lowest form factor of 83.26% is obtained with SPIRO-OMeTAD. In any case, the variation of HTL thickness between 5 nm and 20 nm does not significantly influence the form factor.

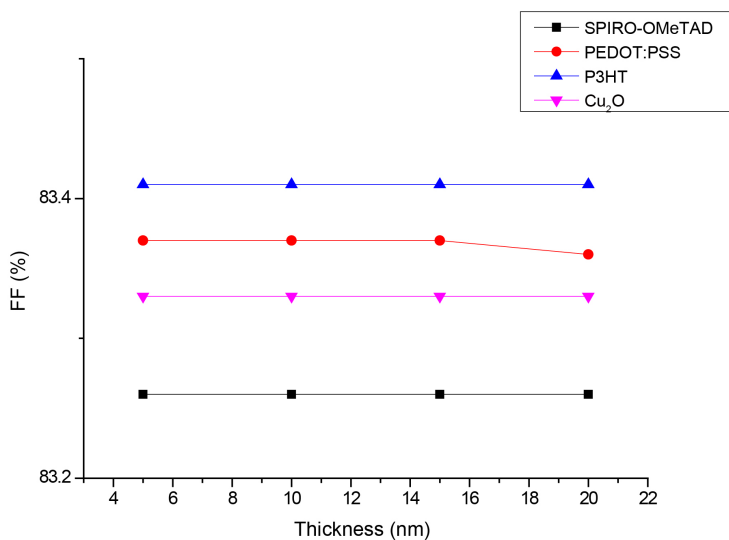


**Figure 5.** Influence of HTL thickness layer (SPIRO-OMeTAD, PEDOT:PSS, P3HT and Cu<sub>2</sub>O) on fill factor.

### 3.2.4. Influence of HTL Thickness Layer on the Power Conversion Efficiency

We can observe the influence of HTL thickness layer (SPIRO-OMeTAD, PEDOT:PSS, P3HT and Cu<sub>2</sub>O) on efficiency in **Figure 6**. As for the other parameters,

the efficiency (PCE) keeps constant values respectable of 35.16% for SPIRO-OMeTAD; 35.19% for P3HT and  $\text{Cu}_2\text{O}$  and 35.21% for PEDOT:PSS. It appears from these analyses that the thickness range considered (5 nm to 20 nm) is not a limiting factor. It is rather the energy alignment and the quality of the interface that determine the performance of the cell. Although the HTL considered in this study compete with almost equal cell performance, they still have intrinsic limits [36]. Indeed, the SPIRO-OMeTAD suffers from instability due to Li-TFSI doping [37]. PEDOT:PSS can corrode the electrodes from the presence of PSS which is acidic and attracts water [38]. As for P3HT, its conductivity is low. It requires appropriate doping to improve its conductivity [38]. Interracial quality and defect management are limits for  $\text{Cu}_2\text{O}$  [39] [40].

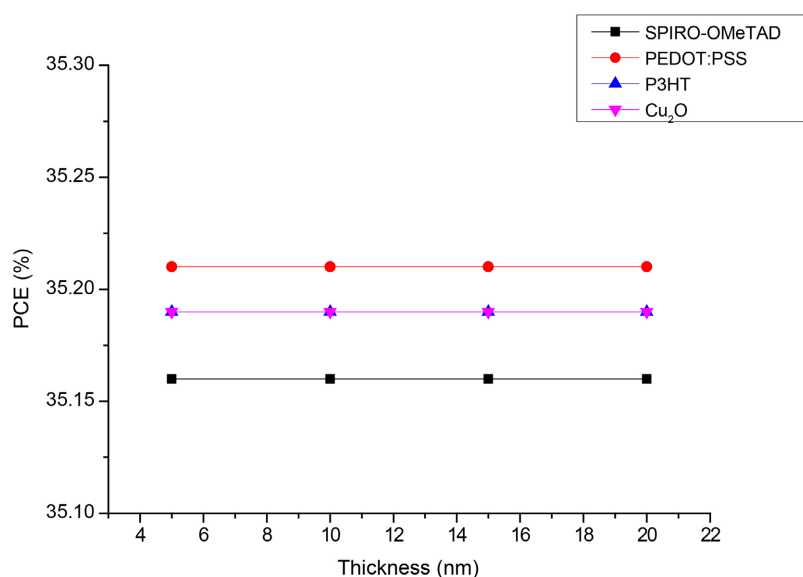


**Figure 6.** Influence of HTL thickness layer (SPIRO-OMeTAD, PEDOT:PSS, P3HT and  $\text{Cu}_2\text{O}$ ) on efficiency.

### 3.3. Influence of Doping Active Layer on Solar Cell Parameters

**Figure 7** shows the influence of doping ( $1 \times 10^{10}$  to  $1 \times 10^{22} \text{ Cm}^{-3}$ ) of the perovskite layer on  $J_{sc}$ ,  $V_{oc}$ , FF and PCE. We considered the perovskite solar cell with Spiro-OMeTAD as the hole transport layer and hematite as the electron transport layer. We notice that when the NA concentration increases from  $1 \times 10^{10}$  to  $1 \times 10^{20} \text{ Cm}^{-3}$ , all the parameters of the cell improve. These improvements are related to a better conductivity of the material, an enhancement of the internal field (which promotes charge separation) and a reduction in series resistance [41] [42].

However, beyond  $1 \times 10^{20} \text{ cm}^{-3}$  and particularly at  $1 \times 10^{22} \text{ cm}^{-3}$ , all parameters drop sharply (PCE  $\approx$  8%). This phenomenon reflects a massive increase in non-radiative recombination and possibly Auger recombination [43]. Excessive displacement of the Fermi level then reduces  $V_{oc}$  and FF, and consequently the yield. The use of hematite as ETL layer with its modest stability and mobility, requires interfacial passivation in order to fully exploit the benefits of optimized doping

[8]. These results are in line with the work of Qureshi *et al.* [34]. To obtain high yields, it is necessary to properly dope the absorber and improve the HTL/Absorber and Absorber/ETL interfaces.

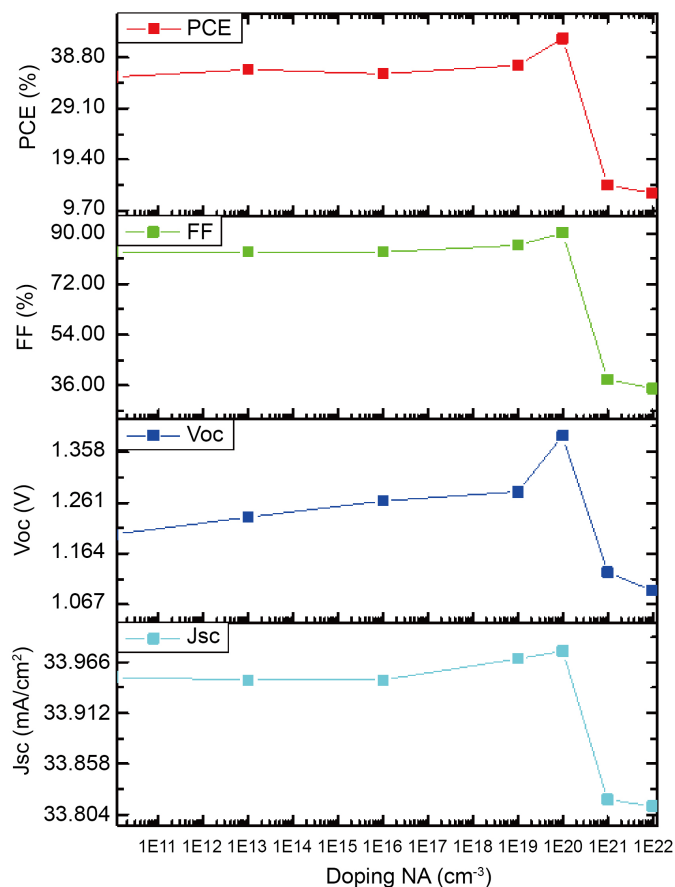


**Figure 7.** Influence of perovskite doping layer on solar cell parameter.

#### 4. Conclusion

In this study, it was the question about simulating the performance of a perovskite solar cell using different types of HTL materials. We first simulated the influence of the thickness of the perovskite on the cell parameters. It appears that the thickness of 700 nm would be the optimal thickness of the perovskite. Then, we explored the effect of the thickness of hole transport layers on the solar cell parameters. We can remember that for the considered thickness range (5 nm to 20 nm), SPIRO-OMeTAD, PEDOT:PSS, P3HT and Cu<sub>2</sub>O contribute separately to having almost equal performances. The major difference lies in the limits of their intrinsic properties. Finally, we simulated the effect of perovskite doping on cell performance. It turns out that performance drops with too much doping. The optimal doping is around  $1 \times 10^{20} \text{ cm}^{-3}$  which allows for a conversion efficiency of more than 42%. Certainly, we have not presented here the influence of the electron transport layer, the hematite, however these results could depend on this layer all

the more so as its mobility and transparency are also factors in the performance of the solar cell. In perspective, the experimental study would enable these theoretical results to be compared with real results and to analyze the stability of different HTL in relation to the performance of the cell.

### Acknowledgements

The authors sincerely thank Dr. Marc Burgelmann and his team at the University of Gent, Belgium, for providing the scientific community with this simulation program.

### Conflicts of Interest

The authors declare no conflicts of interest regarding the publication of this paper.

### References

- [1] Schmela, M., Rossi, R., Lits, C., Chunduri, S.K., Shah, A., Muthyal, R., *et al.* (2023) Advancements in Solar Technology, Markets, and Investments—A Summary of the 2022 ISA World Solar Reports. *Solar Compass*, **6**, Article ID: 100045. <https://doi.org/10.1016/j.solcom.2023.100045>
- [2] Niewelt, T., Steinhäuser, B., Richter, A., Veith-Wolf, B., Fell, A., Hammann, B., *et al.* (2022) Reassessment of the Intrinsic Bulk Recombination in Crystalline Silicon. *Solar Energy Materials and Solar Cells*, **235**, Article ID: 111467. <https://doi.org/10.1016/j.solmat.2021.111467>
- [3] Shahivandi, H. (2025) Understanding Thermal Effects on Band Gap and Absorption in MAPbI<sub>3</sub> Perovskite Solar Cells. *Solid State Sciences*, **168**, Article ID: 108054. <https://doi.org/10.1016/j.solidstatesciences.2025.108054>
- [4] Khir, H., Pandey, A.K., Saidur, R., Ahmad, M.S. and Samykan, M. (2025) Advancements, Challenges and Future Prospects of Flexible Pb-Free Perovskite Solar Cells. *Journal of Power Sources*, **656**, Article ID: 238025. <https://doi.org/10.1016/j.jpowsour.2025.238025>
- [5] Fischer, O., Bett, A.J., Zhu, Y., Messmer, C., Bui, A.D., Schygulla, P., *et al.* (2025) Revealing Charge Carrier Transport and Selectivity Losses in Perovskite Silicon Tandem Solar Cells. *Matter*. <https://doi.org/10.1016/j.matt.2025.102404>
- [6] Jakob, L., Wiedenmann, F., Hanser, M., Schube, J., Bivour, M., Fischer, O., *et al.* (2026) Multifunctional Ti(Al)O<sub>x</sub> Layers for Silver and Indium-Free Perovskite/Silicon Tandem Solar Cells. *Solar Energy Materials and Solar Cells*, **294**, Article ID: 113892. <https://doi.org/10.1016/j.solmat.2025.113892>
- [7] Szymtkowski, J., Huang, C., Bykkam, S., Glowienka, D. and Galagan, Y. (2025) Interface Passivation of a Hole Transporting Material in Order to Improve the Efficiency of Perovskite Solar Cells. *Solar Energy*, **300**, Article ID: 113817. <https://doi.org/10.1016/j.solener.2025.113817>
- [8] Wu, T., Liu, X., Luo, X., Lin, X., Cui, D., Wang, Y., *et al.* (2021) Lead-Free Tin Perovskite Solar Cells. *Joule*, **5**, 863-886. <https://doi.org/10.1016/j.joule.2021.03.001>
- [9] Kim, G., Min, H., Lee, K.S., Lee, D.Y., Yoon, S.M. and Seok, S.I. (2020) Impact of Strain Relaxation on Performance of  $\alpha$ -Formamidinium Lead Iodide Perovskite Solar Cells. *Science*, **370**, 108-112. <https://doi.org/10.1126/science.abc4417>
- [10] Jiang, Q., Zhao, Y., Zhang, X., Yang, X., Chen, Y., Chu, Z., *et al.* (2019) Surface Pas-

- sivation of Perovskite Film for Efficient Solar Cells. *Nature Photonics*, **13**, 460-466. <https://doi.org/10.1038/s41566-019-0398-2>
- [11] Njema, G.G., Kibet, J.K. and Ngari, S.M. (2025) Performance Optimization of a Novel Perovskite Solar Cell with Power Conversion Efficiency Exceeding 37% Based on Methylammonium Tin Iodide. *Next Energy*, **6**, Article ID: 100182. <https://doi.org/10.1016/j.nxener.2024.100182>
- [12] Moyofola, O.O. and Emetere, M.E. (2025) Improving the Performance Conversion Efficiency of Perovskite Solar Cells through Optimization of Charge Transport Layers: A Review. *Renewable and Sustainable Energy Reviews*, **222**, Article ID: 115943. <https://doi.org/10.1016/j.rser.2025.115943>
- [13] Panda, P., Kaur, J., Basu, R., Sharma, A.K., Madan, J. and Pandey, R. (2025) Toward High-Efficiency Photovoltaics: MASnI<sub>3</sub> and FASnI<sub>3</sub> Double Absorber Perovskite Solar Cells with Optimized Conversion Efficiency of 28%. *Physica B: Condensed Matter*, **710**, Article ID: 417232. <https://doi.org/10.1016/j.physb.2025.417232>
- [14] Ghosh, A., Zishan, A.S., Moumita, M., Kumar, Y.A., Roy, A.K., Islam, S., *et al.* (2025) Improving the Performance of AgCdF<sub>3</sub>-Based Perovskite Solar Cells Using Machine Learning-Driven Adjustment of Active Layer and Charge Transport Materials with SCAPS-1D. *Inorganic Chemistry Communications*, **179**, Article ID: 114829. <https://doi.org/10.1016/j.inoche.2025.114829>
- [15] Hsu, C., Kumar, A., Reddy, M.S., Dehghanipour, M., Khorshidi, E., Al-Hasnaawei, S., *et al.* (2025) Emerging Multifunctional Additives in the Perovskite Layer and Its Interfaces with Charge Transport Layers: A Roadmap for Customized Applications in Perovskite Solar Cells. *Journal of Alloys and Compounds*, **1040**, Article ID: 183421. <https://doi.org/10.1016/j.jallcom.2025.183421>
- [16] Lekshmy, R.R., Ammar, M., Ahmad, Z., Shakoor, A., Touati, F., Iwamoto, M., *et al.* (2025) Progress and Challenges in HTL-Free Perovskite Solar Cells. *Solar Energy*, **300**, Article ID: 113831. <https://doi.org/10.1016/j.solener.2025.113831>
- [17] Calió, L., Kazim, S., Grätzel, M. and Ahmad, S. (2016) Hole-Transport Materials for Perovskite Solar Cells. *Angewandte Chemie International Edition*, **55**, 14522-14545. <https://doi.org/10.1002/anie.201601757>
- [18] Chien, H., Pözl, M., Koller, G., Challinger, S., Fairbairn, C., Baikie, I., *et al.* (2017) Effects of Hole-Transport Layer Homogeneity in Organic Solar Cells—A Multi-Length Scale Study. *Surfaces and Interfaces*, **6**, 72-80. <https://doi.org/10.1016/j.surfin.2016.11.008>
- [19] Liu, X., Jiang, X., Wang, K., Miao, C. and Zhang, S. (2022) Recent Advances in Selenophene-Based Materials for Organic Solar Cells. *Materials*, **15**, Article 7883. <https://doi.org/10.3390/ma15227883>
- [20] Bakr, Z.H., Wali, Q., Fakhruddin, A., Schmidt-Mende, L., Brown, T.M. and Jose, R. (2017) Advances in Hole Transport Materials Engineering for Stable and Efficient Perovskite Solar Cells. *Nano Energy*, **34**, 271-305. <https://doi.org/10.1016/j.nanoen.2017.02.025>
- [21] Wang, Y., Luo, Q., Wu, N., Wang, Q., Zhu, H., Chen, L., *et al.* (2015) Solution-Processed MoO<sub>3</sub>:PEDOT:PSS Hybrid Hole Transporting Layer for Inverted Polymer Solar Cells. *ACS Applied Materials & Interfaces*, **7**, 7170-7179. <https://doi.org/10.1021/am509049t>
- [22] Kenfack, A.D.K. and Msimanga, M. (2025) Effect of Low-Cost Hole Transport Layers (HTLs) on the Performance Parameters of Lead-Free Homo Junction CsGeI<sub>2</sub>Br-Based Perovskite Solar Cells. *Next Materials*, **6**, Article ID: 100482. <https://doi.org/10.1016/j.nxmate.2024.100482>

- [23] Tuo, S., Koffi, K.B.M.K., Kamenan, K.A., Datte, J. and Yapi, A.S. (2024) SCAPS 1D Simulation of a Lead-Free Perovskite Photovoltaic Solar Cell Using Hematite as Electron Transport Layer. *Modeling and Numerical Simulation of Material Science*, **14**, 97-106. <https://doi.org/10.4236/mnsms.2024.144006>
- [24] Waychunas, G.A., Kim, C.S. and Banfield, J.F. (2005) Nanoparticulate Iron Oxide Minerals in Soils and Sediments: Unique Properties and Contaminant Scavenging Mechanisms. *Journal of Nanoparticle Research*, **7**, 409-433. <https://doi.org/10.1007/s11051-005-6931-x>
- [25] Burgelman, M., Nollet, P. and Degraeve, S. (2000) Modelling Polycrystalline Semiconductor Solar Cells. *Thin Solid Films*, **361**, 527-532. [https://doi.org/10.1016/S0040-6090\(99\)00825-1](https://doi.org/10.1016/S0040-6090(99)00825-1)
- [26] Patel, P.K. (2021) Device Simulation of Highly Efficient Eco-Friendly  $\text{CH}_3\text{NH}_3\text{SnI}_3$  Perovskite Solar Cell. *Scientific Reports*, **11**, Article No. 3082. <https://doi.org/10.1038/s41598-021-82817-w>
- [27] Berardi, S., Cristino, V., Bignozzi, C.A., Grandi, S. and Caramori, S. (2022) Hematite-based Photoelectrochemical Interfaces for Solar Fuel Production. *Inorganica Chimica Acta*, **535**, Article ID: 120862. <https://doi.org/10.1016/j.ica.2022.120862>
- [28] Mandadapu, U., Thyagarajan, K. and Vedanayakam, S.V. (2017) Simulation and Analysis of Lead Based Perovskite Solar Cell Using SCAPS-1D. *Indian Journal of Science and Technology*, **10**, 1-8. <https://doi.org/10.17485/ijst/2017/v10i11/110721>
- [29] Alkhalzali, A.M. (2019) Investigation the Effect of Post Deposition Thermal Treatment on Properties P3HT and P3HT:PCBM Blend. *Iraqi Journal of Physics*, **17**, 65-75. <https://doi.org/10.30723/ijp.v17i42.439>
- [30] Kunya, S.I., Abdu, Y., Mustafa, M.K. and Ahmad, M.K. (2022) Cuprous Oxide ( $\text{Cu}_2\text{O}$ ) Based Solar Cell Thickness Dependence. *British Journal of Physics Studies*, **1**, 1-7. <https://doi.org/10.32996/bjps.2022.1.1.1>
- [31] Slami, A., Bouchaour, M. and Merad, L. (2019) Numerical Study of Based Perovskite Solar Cells by SCAPS-1D. *International Journal of Energy and Environment*, **13**, 17-21.
- [32] Akel, S., Kulkarni, A., Rau, U. and Kirchartz, T. (2023) Relevance of Long Diffusion Lengths for Efficient Halide Perovskite Solar Cells. *PRX Energy*, **2**, Article ID: 013004. <https://doi.org/10.1103/prxenergy.2.013004>
- [33] Oishi, A.H., Anjum, M.T., Islam, M.M. and Nayan, M.F. (2023) Impact of Absorber Layer Thickness on Perovskite Solar Cell Efficiency: A Performance Analysis. *European Journal of Electrical Engineering and Computer Science*, **7**, 48-51. <https://doi.org/10.24018/ejece.2023.7.2.520>
- [34] Qureshi, A.A., Javed, S., Akram, M.A., Schmidt-Mende, L. and Fakharuddin, A. (2023) Solvent-Assisted Crystallization of an  $\alpha\text{-Fe}_2\text{O}_3$  Electron Transport Layer for Efficient and Stable Perovskite Solar Cells Featuring Negligible Hysteresis. *ACS Omega*, **8**, 18106-18115. <https://doi.org/10.1021/acsomega.3c01405>
- [35] Bouderbala, I.Y. and Hamdi, N.H. (2023) Effects of Absorber Layer Thickness and Doping Density on the Performance of Perovskite Solar Cells: A Simulation Analysis Using SCAPS-1D Software. *Algerian Journal of Research and Technology*, **8**, 131-137.
- [36] Rakstys, K., Igci, C. and Nazeeruddin, M.K. (2019) Efficiency vs. Stability: Dopant-Free Hole Transporting Materials Towards Stabilized Perovskite Solar Cells. *Chemical Science*, **10**, 6748-6769. <https://doi.org/10.1039/c9sc01184f>
- [37] Cameron, J. and Skabara, P.J. (2020) The Damaging Effects of the Acidity in PE-

- DOT:PSS on Semiconductor Device Performance and Solutions Based on Non-Acidic Alternatives. *Materials Horizons*, **7**, 1759-1772.  
<https://doi.org/10.1039/c9mh01978b>
- [38] Li, S., Cao, Y., Li, W. and Bo, Z. (2021) A Brief Review of Hole Transporting Materials Commonly Used in Perovskite Solar Cells. *Rare Metals*, **40**, 2712-2729.  
<https://doi.org/10.1007/s12598-020-01691-z>
- [39] Lin, C., Liu, G., Xi, X., Wang, L., Wang, Q., Sun, Q., *et al.* (2022) The Investigation of the Influence of a Cu<sub>2</sub>O Buffer Layer on Hole Transport Layers in MAPbI<sub>3</sub>-Based Perovskite Solar Cells. *Materials*, **15**, Article 8142.  
<https://doi.org/10.3390/ma15228142>
- [40] Yousuf, M.H., Saeed, F. and Tauqeer, H.A. (2022) Numerical Investigation of Cu<sub>2</sub>O as a Hole Transport Layer for High-Efficiency, Cadmium Free CIGS Solar Cell.  
<https://doi.org/10.20944/preprints202110.0326.v2>
- [41] Ahamad, M. and Hossain, A.K.M.A. (2023) Design and Optimization of Non-Toxic and Highly Efficient Tin-Based Organic Perovskite Solar Cells by Device Simulation. *Heliyon*, **9**, e19389. <https://doi.org/10.1016/j.heliyon.2023.e19389>
- [42] Liang, J., Wang, Y., Liu, X., Chen, J., Peng, L. and Lin, J. (2024) Theoretical Analysis of Doping of Perovskite Light-Absorbing Layer for Highly Efficient Perovskite Solar Cells. *Journal of Physics and Chemistry of Solids*, **188**, Article ID: 111901.  
<https://doi.org/10.1016/j.jpics.2024.111901>
- [43] Sinha, N.K., Roy, P., Ghosh, D.S. and Khare, A. (2023) Investigation of Effect of Doping in Perovskite Solar Cells: A Numerical Simulation Approach. *Materials Today: Proceedings*, **83**, 6-13. <https://doi.org/10.1016/j.matpr.2022.10.006>